Progress in Disaster Science 5 (2020) 100062

Contents lists available at ScienceDirect

Progress in Disaster Science

journal homepage: www.elsevier.com/locate/pdisas

Monitoring progress of the Sendai Framework using a geospatial model: The example of people affected by agricultural droughts in Eastern Cape, South Africa

Yvonne Walz [a,*], Annika Min [a], Karen Dall [a], Moses Duguru [b], Juan-Carlos Villagran de Leon [b], Valerie Graw [c], Olena Dubovyk [c], Zita Sebesvari [a], Andries Jordaan [d], Joachim Post [e]

[a] United Nations University – Institute for Environment and Human Security (UNU-EHS), Bonn, Germany
[b] United Nations Space-Based Information for Disaster Management and Emergency Response (UN-SPIDER), Bonn, Germany
[c] Rheinische Friedrich-Wilhelms University Bonn – Center for Remote Sensing of Land Surfaces (ZFL), Bonn, Germany
[d] University of the Free State – Disaster Management Training and Education Centre for Africa (DiMTEC), Bloemfontein, South Africa
[e] German Aerospace Center (DLR), Cologne, Germany

ARTICLE INFO

Article history:
Received 26 May 2019
Received in revised form 26 November 2019
Accepted 3 December 2019
Available online 06 December 2019

Keywords:
Monitoring
Sendai Framework
Affected people
Disaster risk reduction
Drought
South Africa

Keywords:
Monitoring
Sendai Framework
Affected people
Disaster risk reduction
Drought
South Africa

ABSTRACT

The Sendai Framework for Disaster Risk Reduction (SFDRR) was adopted by 187 countries and offers a tangible agenda for evidence-based policy for disaster risk reduction as an integral part of the overall post-2015 global development agenda. The progress of implementation of the seven Global Sendai Targets at the national level is tracked by a set of 38 indicators. However, despite the formal commitment, the majority of countries is currently not in the position to monitor the implementation of the Global Targets. The lack of information on disaster-related loss and damage is mainly due to gaps in data availability, quality, and accessibility, which impairs an accurate, timely and high quality monitoring process. This research addressed this gap by developing a model approach, which aimed at "translating" indicators described by the technical guidance of the United Nations Office for Disaster Risk Reduction (UNDRR) into a geospatial procedure which builds on remote sensing data, climate data, land cover and land use data, agricultural statistics and population census data. With this geospatial model approach, we quantified indicators of the SFDRR for Target B "number of people affected" for the example of agricultural drought in the Eastern Cape province of South Africa in a spatially explicit way. We conducted a media content analysis to generate proxy reference data for evaluation of the model results. In addition, we explored the sensitivity of the model using three different input data on drought hazard, namely the Vegetation Condition Index (VCI), the Standard Precipitation Evapotranspiration Index (SPEI) and the combination of these. The spatial distribution of number of people affected corresponded very well with reference data from the media content analysis; however, model results were very sensitive to different hazard input data. This geospatial model based on remote sensing and geostatistical data is to the best of our knowledge the first attempt to measure Sendai indicators in the absence of national loss and damage databases and provides a unique opportunity to support many countries in implementing the framework. Due to its retrospective nature, even a baseline measure of the indicators can be derived as a reference for monitoring progress. However, the model needs to be further validated in order to qualify the underlying assumptions made to determine thresholds of people being affected. Future research should transfer this model to different hazard contexts to allow hazard-specific monitoring of loss and damage in order to develop targeted disaster risk reduction measures.

1. Introduction

In March 2015, the United Nations Sendai Framework for Disaster Risk Reduction (SFDRR) was adopted by 187 countries with the aim to protect lives, livelihoods, ecosystems, and critical infrastructure from natural and human-caused hazards over the next 15 years [62,73,76]. To achieve this ambitious goal, the global community identified and agreed upon a set of seven Global Targets and four Priorities for Action, fostering the shift from managing disasters to managing disaster risk through understanding risk, reducing existing risk, preventing new risk and strengthening societal and environmental resilience [73]. In this sense, the SFDRR offers a tangible agenda for evidence-based policy and connects with other pillars of the post 2015 global development agenda, such as the United Nations Sustainable Development Goals (SDGs) [63], the Paris Agreement to reduce climate change and its impacts [65] and the New Urban Agenda [60] through the common notion of resilience [46]. Following the successful adoption of the SFDRR, the signatory countries face diverse challenges to implement

* Corresponding author at: Platz der Vereinten Nationen 1, 53113 Bonn, Germany.
E-mail address: walz@ehs.unu.edu. (Y. Walz).

http://dx.doi.org/10.1016/j.pdisas.2019.100062

the framework, which also calls for scientific support specifically for measuring and advancing the quantitative targets [2,9,41].

The open-ended intergovernmental expert working group on indicators and terminology relating to disaster risk reduction (OIEWG-DRR) has developed 38 indicators to monitor progress of the seven Global Targets of the SFDRR [61,71], which simultaneously inform several targets of the SDGs (SDG#1, #11, #13) [66]. The indicators should be measured at the national level and reported by countries on a yearly basis through the "*Sendai monitor*"[1], a web-based system that was launched by the United Nations Office for Disaster Risk Reduction (UNISDR) in March 2018. The main aim of the *Sendai monitor* is to quantify progress of the Global Targets and thereby improve the understanding of underlying causes of loss and damage due to disasters. To contribute to the implementation of the SFDRR, this information will be monitored and form the basis of new targeted measures to reduce disaster risks and impacts. Against this background, countries were requested in the year 2018 to measure indicators of the Global Targets from 2015 to 2017 and to derive the baseline data for the years 2005–2015 for Targets A and B by April 2019 [67]. As of May 2019, 196 countries are registered to report to the *Sendai monitor*; however, between 184 and 196 countries - depending on the target and the year - have not started at all with the reporting process for the period 2015–2017 [68].

The technical guidance on data and methodologies for measuring the targets and indicators of the SFDRR [71] provides the basis to support the countries in the implementation of the SFDRR. However, a country-based survey has identified a range of scientific and technological needs to be addressed during the process of drafting and negotiating the SFDRR to realize its implementation [9]. In addition, a global review on data reporting for the indicators of the SFDRR has shown that critical gaps exist in disaster loss data and confirms that "unless gaps in data availability, quality, and accessibility are addressed, countries' ability to assure accurate, timely and high quality monitoring and reporting of implementation across all Targets and Priorities of the Sendai Framework will be severely impaired" [72: p75]. This lack of data is confirmed by the latest statistics of the global *Inventory system of the effects of disasters* database DesInventar[2], which has a direct interface with the *Sendai monitor* [70]. In the database, merely 18 of 104 registered countries are being updated in near-real time and only around 50 countries have loss and damage data spanning the years 2005 to 2015. Thus, the majority of countries has to deal with a lack of data and capacity both for measuring the indicators of the SFDRR and, even more so, to retrospectively establish the baseline for monitoring progress of the Global Targets.

South Africa represents one of many countries where disasters are reported but no national database on loss and damage has yet been established [68]. Quantification of impacts due to major disaster events is often conducted only by individual sectors such as agriculture or water affairs [47]. Due to lack of a comprehensive, standardized, and hazard-specific loss and damage monitoring system, the National Disaster Management Center (NDMC) of South Africa confirms that reporting for the Sendai Monitor at the national level is currently not feasible for the country [42].

Droughts are considered the most relevant hazard in terms of economic losses in South Africa and many other areas around the globe [69]. They are recurring, slow-onset hazards, belong to the most widespread climate extremes, are projected to increase in magnitude and frequency, and cause major impacts on human and natural systems [10,48]. The agricultural sector is in many regions the key economic factor and basis for livelihoods, yet highly vulnerable to climate-related hazards [19]. A review of post disaster needs assessments revealed that worldwide 83% of agricultural loss and damage between 2006 and 2016 was attributed to droughts, of which the losses alone amounted to over 29 billion US$ (ibid). While droughts cause large-scale economic losses in industrialized regions, the societal impact is most severe in least developed countries, where basic income and food security directly depends on agricultural outputs with a high ratio of subsistence farming [10].

In South Africa, the agricultural sector is experiencing severe impacts due to droughts. Accounting for approximately 60% of overall water demand, it is the largest user of water in South Africa [47]. At the same time, the livestock sector is the largest contributor to total agricultural gross domestic product, producing about 48% of South Africa's agricultural output in terms of value [20]. Drought events in South Africa usually correlate with El Niño years, which also holds true for the severe drought in 2015/16 [40]. While South Africa is typically a net exporter of food, the 2015/16 drought turned the country into a net importer [1,4]. Moreover, this specific drought event led to increased unemployment and substantial water restrictions in many regions of the country [4]. However, no systematic information about the number of people affected by the drought or corresponding economic losses is available, as would be necessary for the *Sendai monitor* and to progress with the implementation of the SFDRR.

Recent research demonstrates that earth observation data can play a key role in achieving the post-2015 global development agenda, particularly by supporting the quantification of indicators for monitoring the achievement of respective targets [3,39,45]. Geospatial approaches using earth observation data in combination with other spatial data such as soil characteristics, area of irrigated agriculture and people exposed have been developed in the context of agricultural drought risk [49,75]. The Global Drought Observatory (GDO) is to our knowledge the most relevant and recent initiative, where drought risk assessment is used to estimate drought-related impacts on the agricultural sector at the global level [75]. However, there are currently no approaches that result the number of people affected as needed for monitoring Target B of the SFDRR.

Against this background, this research develops and investigates a geospatial model approach using satellite remote sensing data in combination with agricultural and demographic statistics in order to derive a quantitative estimate of the number of people affected (= indicator B-5 of the SFDRR) for the example of agricultural drought in South Africa in the year 2015/2016. The overall aim is to better understand the opportunities and challenges of this geospatial model approach to overcome the lack of loss and damage data, provide an alternative solution for monitoring progress of the Global Targets of the SFDRR, and support improvements in disaster risk reduction in countries like South Africa. The specific objectives of this paper are (i) to present the developed geospatial model approach using remote sensing and geostatistical data for measuring indicator B-5 for the example of agricultural drought in the Eastern Cape province of South Africa, (ii) to test the sensitivity of the model and evaluate the results based on different hazard input data and impact data from a newspaper content analysis, and (iii) to discuss the opportunities and limitations of this approach for (retrospectively) assessing SFDRR indicators to establish a baseline and to advance disaster risk reduction.

2. Material and methods

2.1. Study area: Eastern Cape Province, South Africa

The Eastern Cape province is located in the southern coastal area of South Africa (Fig. 1). Here, agriculture is an important source of income and livelihood for >35% of the households in mainly rural areas [14,54,55]. It was selected as the case study area for the following reasons: (i) the complete province was affected by the 2015/2016 drought in South Africa, (ii) the proportion of households dependent on agriculture is highest in Eastern Cape out of all South African provinces, (iii) the province contains eight of the nine biomes of South Africa, and (iv) the study area represents a large rainfall gradient ranging from 250 mm to 1000 mm per year [53].

The latest census documented 6.5 million people living in the Eastern Cape province [56]. Despite the overall population increase in South Africa between 2001 (44.8 million) and 2017 (56.7 million), the Eastern Cape province experienced the highest population decrease among all provinces of SA during this period, mainly due to outmigration to other provinces with better economic opportunities

[1] https://sendaimonitor.unisdr.org/.
[2] https://www.desinventar.org/.

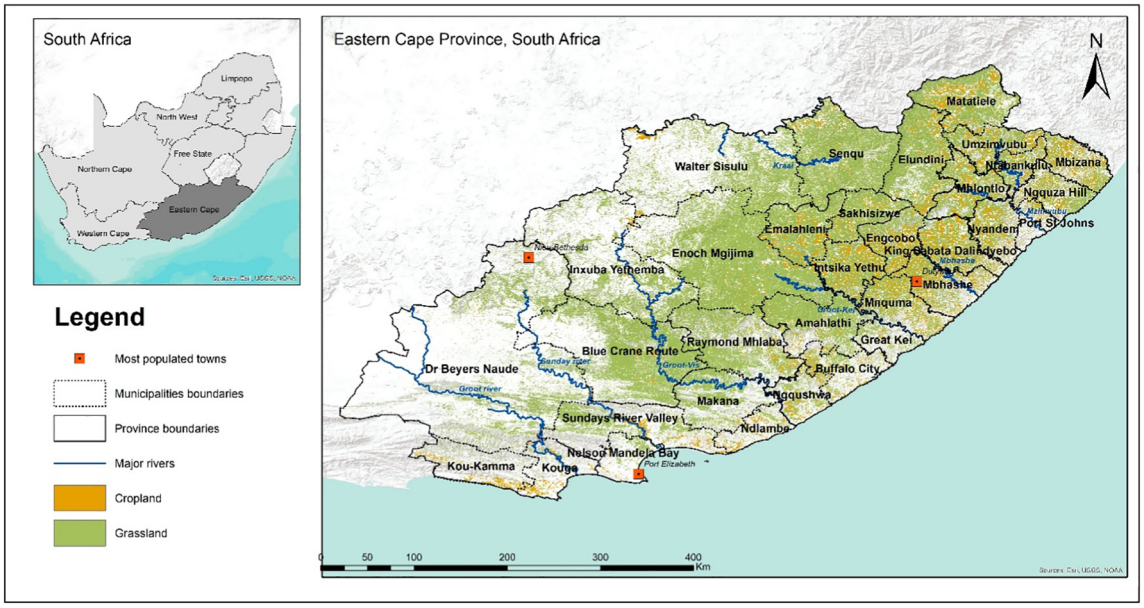

Fig. 1. Overview of the study area – Eastern Cape province in South Africa. Data sources: rivers: Department of Water and Sanitation, South Africa – Strahler level 4 and 5 displayed here; crop-/grassland: Department of Environmental Affairs – classes of crop and grassland displayed here.

[56,79]. With regard to agricultural land, approximately 80% of the land is used for natural grazing, mainly for cattle and sheep, with the rest constituting cropland [14,44,54,55]. The study area has a historical demarcation of communal land, which is predominantly rainfed and of which large areas are still managed by tribal authorities with mainly common property right systems [31,33]. At the same time, there are

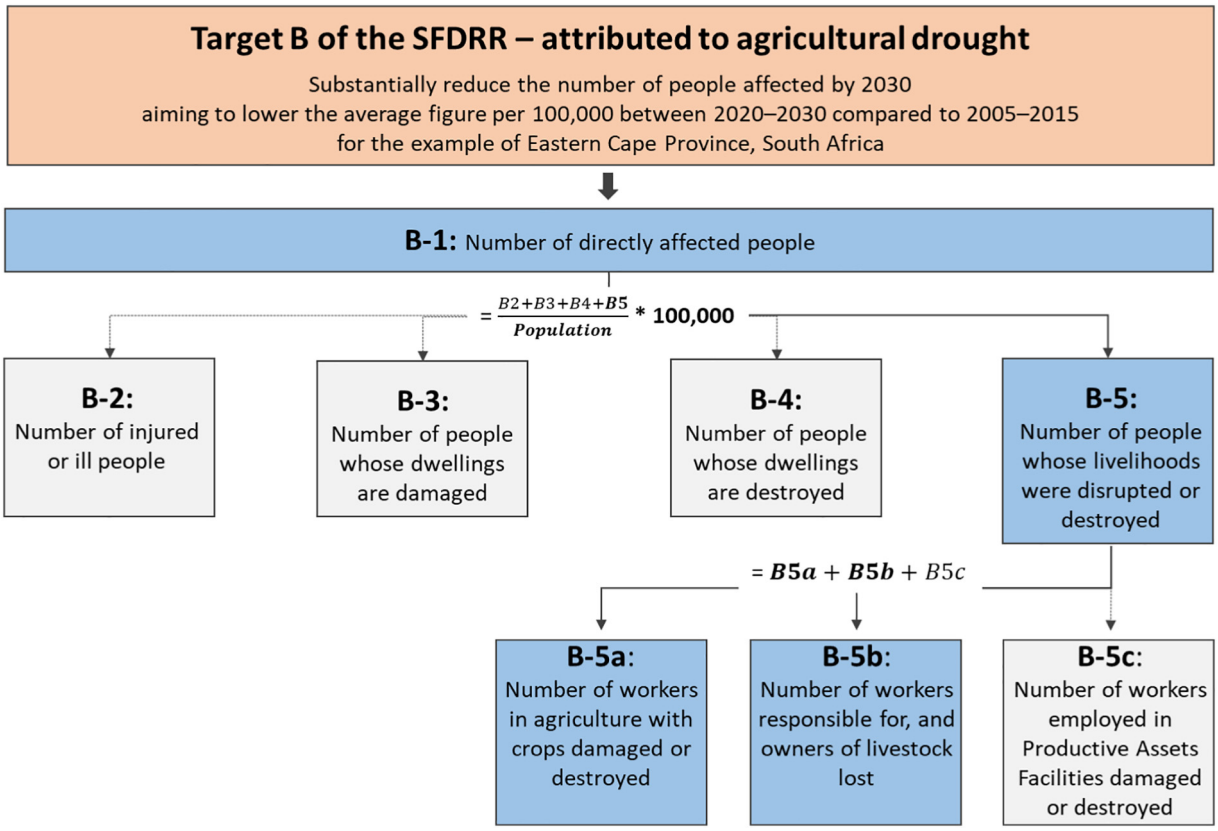

Fig. 2. Methodological approach to monitor Sendai Target B for the example of agricultural drought, adjusted from [71]; grey boxes with dotted arrows represent indicators that are not considered relevant for the context of agricultural drought due to its slow-onset characteristic, whereas blue boxes with solid arrows are included in the assessment of Target B for the given context. (For interpretation of the references to color in this figure legend, the reader is referred to the web version of this article.)

areas with well-planned commercial farms, where individual or private property right systems are well-defined and irrigated farming practices are common (ibid).

2.2. Deriving Sendai Indicator B-5 for agricultural drought

The aim of Sendai Target B is to "substantially reduce the number of affected people globally by 2030, aiming to lower the average global figure per 100,000 between 2020–2030 compared to 2005–2015" ([73]: 12). Fig. 2 illustrates the methodological approach of measuring indicators to monitor Target B for the example of agricultural drought, which consists of five indicators B-1 to B-5 as documented by the Technical Guidelines of UNISDR [71]. However, indicator B-1, which constitutes the number of directly affected people per 100,000 people, is designed as the sum of indicators B-2 to B-5 [71]. As drought is a slow onset hazard, indicators B-2 (number of injured people), B-3 (number of damaged dwellings) and B-4 (number of destroyed dwellings) were not considered relevant in this study. As such, B-1 is equal to B-5 in the drought-specific approach of this study. Indicator B-5 represents the "number of people whose livelihoods were disrupted or destroyed, attributed to disasters" [71: p20], and is considered to be the key indicator for measuring progress of Target B for the example of agricultural droughts. The following two sub-indicators were considered relevant to measure indicator B-5 for the given hazard context: (i) B-5a measures the number of workers in agriculture with crops damaged or destroyed; and (ii) B-5b indicates the number of workers in agriculture with livestock losses attributed to agricultural drought. The third sub-indicator, namely B-5c, measures the number of workers employed in productive asset facilities damaged or destroyed, which could refer to revenue losses and employment of people in e.g. factories for fertilizers or other agricultural products. To measure this indicator, a simple assessment approach is critical, because information is dispersed and would need to be drawn from a wide range of sectors [12]. In this study we focus only on primary agricultural production and do not consider upstream or downstream industries that support agricultural production, and therefore do not consider the indicator B-5c.

Following the technical guidance of the OIEWG-DRR, livelihoods are defined as "capacities, productive assets (both living and material) and activities required for securing a means of living, on a sustainable basis" [71: p21]. The quantitative measure of disrupted or destroyed livelihoods for the example of agricultural drought is derived from the sum of indicators B-5a and B-5b (Fig. 2). For reporting indicator B-5 to the Sendai Monitor, most countries have no in situ data available and need to compute the respective sub-indicators using the following equations as proposed by UNISDR [71]:

$$\mathrm{B-5a} = \text{hectares of crops affected} * \text{average workers per hectare} \quad (1)$$

$$\mathrm{B-5b} = \text{Livestock lost} * \text{average workers per livestock} \quad (2)$$

It should be noted that these equations prescribed by UNISDR are not exhaustive; other variations are possible with respect to data availability and preferred country methodology [71]. In addition, variables to compose these indicators also serve as input for other indicators of the SFDRR. In this case study, we follow this proposed methodology of UNISDR and discuss its strengths and limitations based on the results achieved.

For the example of Eastern Cape in South Africa, we have developed a geospatial model approach to measure the number of people affected by the agricultural drought to inform the Sendai Target B for the time period from July 2015 to June 2016, when a serious drought hit the region. In the following sections, the individual steps from assessing agricultural drought hazard to measuring the respective indicators and evaluating the results are documented.

2.2.1. Assessment of agricultural drought hazard

Agricultural drought emerges when the soil moisture availability to plants has dropped to such a level that it adversely affects the crop yield and hence agricultural profitability [34]. In this study, three different hazard products have been explored with the main aim to investigate the impact of different input data on the resulting number of people affected and understand the sensitivity of the geospatial model approach.

The assessment of agricultural drought hazard, which aims to measure the vegetation response to drought conditions for a given time period, is used to assess hectares of crops affected to measure indicator B-5a. In the absence of in situ data on livestock losses, we measured the vegetation condition of grassland and used this as proxy variable to assess areas of affected livestock and inform the variable of livestock lost as part of indicator B-5b. The assumption was that drought-affected grassland is directly related to livestock loss.

In this study, the satellite remote sensing vegetation index data product (MOD13Q1) from the Moderate Resolution Imaging Spectroradiometer (MODIS) with 16-day temporal and 250 m spatial resolution was used for the period 2000 to 2017. This data was used to assess agricultural drought hazard severity based on the Vegetation Condition Index (VCI) [35] for cropland and grassland in the study area. The VCI is one of the most frequently applied indices to quantify agricultural drought hazard severity [27]. The index ranges from 0 to 100 and is calculated as follows:

$$VCI = 100 * \frac{(EVI - EVI_{min})}{(EVI_{max} - EVI_{min})} \quad (3)$$

where EVI stands for Enhanced Vegetation Index, which measures greenness and is thereby related to health of the vegetation as well as vegetation productivity [18,22]. The annual VCI was calculated using seasonal metrics of vegetation phenology for each growing season in the study region. Here, a weighted linear regression (WLC) scheme was applied to account for crop growing stages vulnerable to drought, as drought impacts on crop growth are more severe during the peak of growing season as well as between the start of the season and the peak of the growing season [77]. Validation of the final product with soil moisture data showed that applying the WLC to the VCI resulted in more accurate drought severity information per year as compared to more generalized annual products [23].

Table 1 presents the classification of the VCI-based drought hazard severity using a commonly applied classification scheme as defined in the literature [7,29] and applied by the U.S. National Drought Mitigation Center [58]. We followed the requirements of the SFDRR by discriminating between "crops damaged or destroyed" by adjusting the VCI-based drought hazard severity classes in line with the drought severity description proposed by Jordaan et al. [31,33] and Jordaan [29]. Accordingly, no impact on crops is assumed where values in crop- and grassland exceed VCI > 40. Damaged crops were related to VCI values below 40, and destroyed crops to a VCI of below 10 (Table 1).

In most cases, agricultural droughts are closely related to and viewed as a result of meteorological droughts, where the amount of rainfall is below normal [31,33,78]. In this study, we used the Standard Precipitation Evapotranspiration Index (SPEI) as an additional drought hazard indicator. The SPEI is derived from both precipitation and temperature data as it considers evapotranspiration, which is the second most significant component of the hydrological budget after precipitation [74]. The SPEI-6 data for March 2016 was downloaded from the Global Drought Monitor with 0.5 degrees spatial resolution and as a six month aggregated product [5,74]. It represents the period from October 2015 to March 2016. The SPEI-based drought severity is, similarly to the VCI, classified based on defined thresholds [11,38,59].

In addition to the individual VCI and SPEI hazard products, a combined VCI and SPEI hazard product was derived to measure the indicator B-5. In a first step, the SPEI data were adjusted to the spatial resolution of the VCI data through spatial disaggregation using the nearest neighbor resampling method. Then, the classified VCI and SPEI products, each with a range between 1 and 5 representing drought severity from D0 to D4 (Table 1), were aggregated using an additive function. The resulting data (ranging from 1 to 10) was then re-classified into five classes of drought hazard severity with equal intervals, and further aggregated into three classes H0

Table 1
Overview of thresholds used for the drought hazard assessment for VCI, SPEI, and the resulting classes of the combined VCI/SPEI data [8,11,29]. *Class values result from the combination of classified VCI and SPEI data ranging from 1 to 5; values in brackets indicate the original value after aggregation, which were then re-classified into five classes ranging from 1 to 5.

Description of drought hazard severity class	Drought hazard severity class	VCI value	SPEI value	Aggregated VCI/SPEI data class value*	Hazard category for Sendai monitoring
No drought	D0	>40	≥ −0.5	1 (1–2)	H0 (crops not affected)
Mild drought	D1	>30–40	−1.0 to < −0.5	2 (3–4)	H1
Moderate drought	D2	>20–30	−1.5 to < −1.0	3 (5–6)	(crops damaged)
Severe drought	D3	10–20	−2.0 to < −1.5	4 (7–8)	
Extreme drought	D4	<10	≤ −2.0	5 (9–10)	H2 (crops destroyed)

to H2. Table 1 summarizes all thresholds of drought hazard indicators used in this study and links the individual drought severity classes to the hazard categories as required by the Sendai indicator B-5, namely H0 (crops not affected), H1 (crops damaged) and H2 (crops destroyed).

2.2.2. Measuring number of people affected due to agricultural drought

The measure of number of people affected due to agricultural drought was derived by combining the results of the drought hazard assessment (2.2.1) with land cover and land use data, agricultural statistics, and population census data (Fig. 3). The 30 m-resolution land cover and land use data were provided by the South African Department of Environmental Affairs [16], and the respective classes were extracted for cropland (#10 to #31) and grassland (#7) [21]. The number of households involved in crop and livestock production, respectively, were provided by the most recently available agricultural household survey at the local municipality level [54]. These data were transformed into the crop- and livestock-dependent populations by multiplying by the average number of people per household from the latest community survey [52]. The next steps towards the calculation of indicator B-5a and B-5b were to spatially overlay the cropland and grassland areas with the drought hazard severity classification and extract the area of exposed crop-/grassland per severity class. In order to link the number of crop-/livestock dependent population to the affected crop-/grassland, we calculated the density of crop-/livestock dependent population per area of crop-/grassland, respectively. Multiplying this density by the respective areas per hazard severity class for crop-/grassland resulted in the number of affected people, which was then normalized per 1000 inhabitants at the local municipality level and aggregated for the EC province. The sum of B-5a and B-5b resulted in Sendai indicator B-5 (see Fig. 2).

Due to different drought hazard datasets, we generated VCI-based, SPEI-based and combined VCI/SPEI-based calculations of the Sendai indicators B-5a, B-5b and B-5. The indicator measure is based on the assumption that the characteristics “crops damaged or destroyed” for Sendai indicator B-5a and “livestock dependent population affected” for B-5b are met when classes H1 or H2 are detected by the drought hazard severity assessment.

It has to be mentioned that there is a large mismatch in spatial resolution between the land use data (30 m resolution), VCI (250 m resolution) and SPEI (0.5°), which impedes the establishment of a direct relationship between the two different drought-related datasets. For processing, all data were resampled to 30 m resolution and then aggregated to the administrative level of local municipalities.

2.2.3. Evaluation of the indicator measurement

Ideally, the most appropriate reference data to evaluate the developed geospatial model approach would be actual loss and damage data collected in situ of people affected in EC during the 2015/2016 drought event. However, as aforementioned, an alternative model approach is urgently needed precisely because of the unavailability of comprehensive and standardized loss and damage data. Against this background, validation of the geospatial model is limited.

For this specific drought event in 2015/2016, the available loss and damage data consisted of 43 declarations of drought events, which were reported by local municipalities and/or the provincial disaster management centre of Eastern Cape according to the Disaster Management Act of South Africa [17]. Droughts were declared for the complete area of the Eastern Cape province, making for a very useful reference for drought occurrence in the respective time frame of this study. However, information regarding drought occurrence is binary without differentiation based on severity; therefore, this data did not qualify for evaluation of the estimated Sendai indicators.

In the absence of detailed loss and damage data for this drought event in the Eastern Cape province, we derived proxy data for the evaluation of the indicator measure based on a content analysis of newspapers from the region. This newspaper content analysis selected six online newspapers in English language relevant for Eastern Cape province in South Africa, namely “Daily Dispatch”, “Go!&Express”, “Grocotts Mail”, “The Herald”, “jBaynews”, and “EC provincial treasury”. We explored their content which spanned the period from July 2015 until June 2016 to cover the complete year using the search term “drought”. Articles were considered relevant if (i) they provided a spatial information linked to the Eastern Cape province and (ii) any impact information was provided and attributed to the drought event in the 2015/2016 timeframe. Based on these criteria, 23 articles were identified as relevant for in-depth analysis and a total of 91 impacts were reported within these articles. In a first step, the number of reported impacts was assigned to and summed up within the respective local municipalities. In a second step, reported impacts were classified in reference to the respective description of impacts as provided with the drought severity classification of Jordaan [29], which also corresponds to the classes defined in Table 1.

An aggregated evaluation index was derived from individual evaluation data sets, namely (i) the number of impacts and (ii) the severity of impacts reported in newspaper articles using the additive multi-criteria analysis approach with equal weighting [6]. As a preparatory step, these data sets were individually classified into classes of low (1), moderate (2) and high (3) impact, indicating whether the respective values fall under the first, second or third tercile of the maximum value for the respective data set.

The evaluation of the resulting Sendai indicators consisted of the following two steps: first, the coefficient of variation was calculated for each local municipality to analyse the heterogeneity between the different values of the indicator B-5 that result from using different hazard input data. Second, the individual B-5 Sendai indicators were analysed in reference to the individual evaluation variables derived from the newspaper content analysis as well as the aggregated evaluation index. The statistical analysis was based on the Spearman

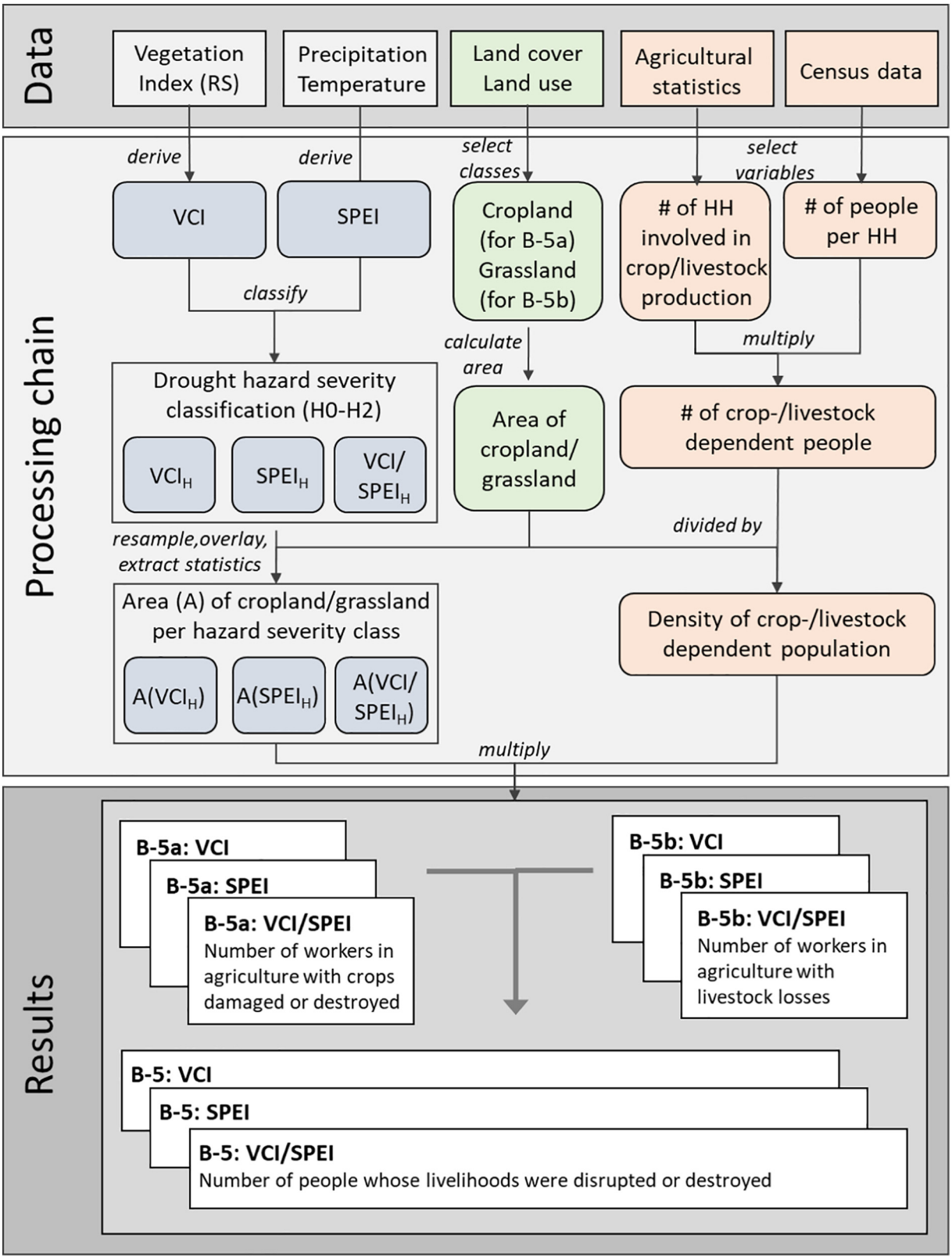

Fig. 3. Geospatial model approach developed to measure number of people affected due to agricultural drought for the case study of Eastern Cape Province, South Africa. This model presents the key input data and steps for processing and integrating data to estimate the respective Sendai indicators. Due to the three different hazard-related input data, three respective measures result per Sendai indicator. Input data for this geospatial model approach are: MOD13Q1 data from MODIS for vegetation index, SPEI-6 data of March 2016 for the precipitation and temperature measure, grass- and cropland classes from a land-use classification, and agriculture-dependent households and people from agricultural statistics and census data. The details of the input data used and procedures as applied for this case study are described in the methods section. HH = Household, RS = Remote Sensing.

rank correlation analysis and the analysis of agreement between the derived indicators and the evaluation data using the Kappa interrater agreement [51].

3. Results

3.1. Estimation of Sendai indicator B-5 for agricultural droughts in Eastern Cape

This study has developed a geospatial model approach (Fig. 3) to measure indicators for monitoring Target B of the SFDRR for the example of agricultural drought in the case study area of the Eastern Cape province of South Africa. The analysis resulted for the year 2015/2016 in the estimated overall number of people affected, which ranged between 12,650 (SPEI-based), 12,911 (VCI/SPEI-based) and 19,667 (VCI-based) affected people per 100,000 inhabitants in the Eastern Cape province as a whole. The developed geospatial model resulted in a calculation of the Sendai indicator B-5 as an aggregated product from indicators B-5a and B-5b, and with that provides the relevant measure to monitor Target B following the guidelines of the *Sendai monitor* for the example of agricultural drought.

Fig. 4 illustrates the results of indicators B-5a, B-5b and B-5 based on the three different drought hazard data. The spatial distribution of the number of affected people varies distinctly by region. In the south-western area of the Eastern Cape province, where population density is also lowest, a low measure of affected people was consistent across local municipalities.

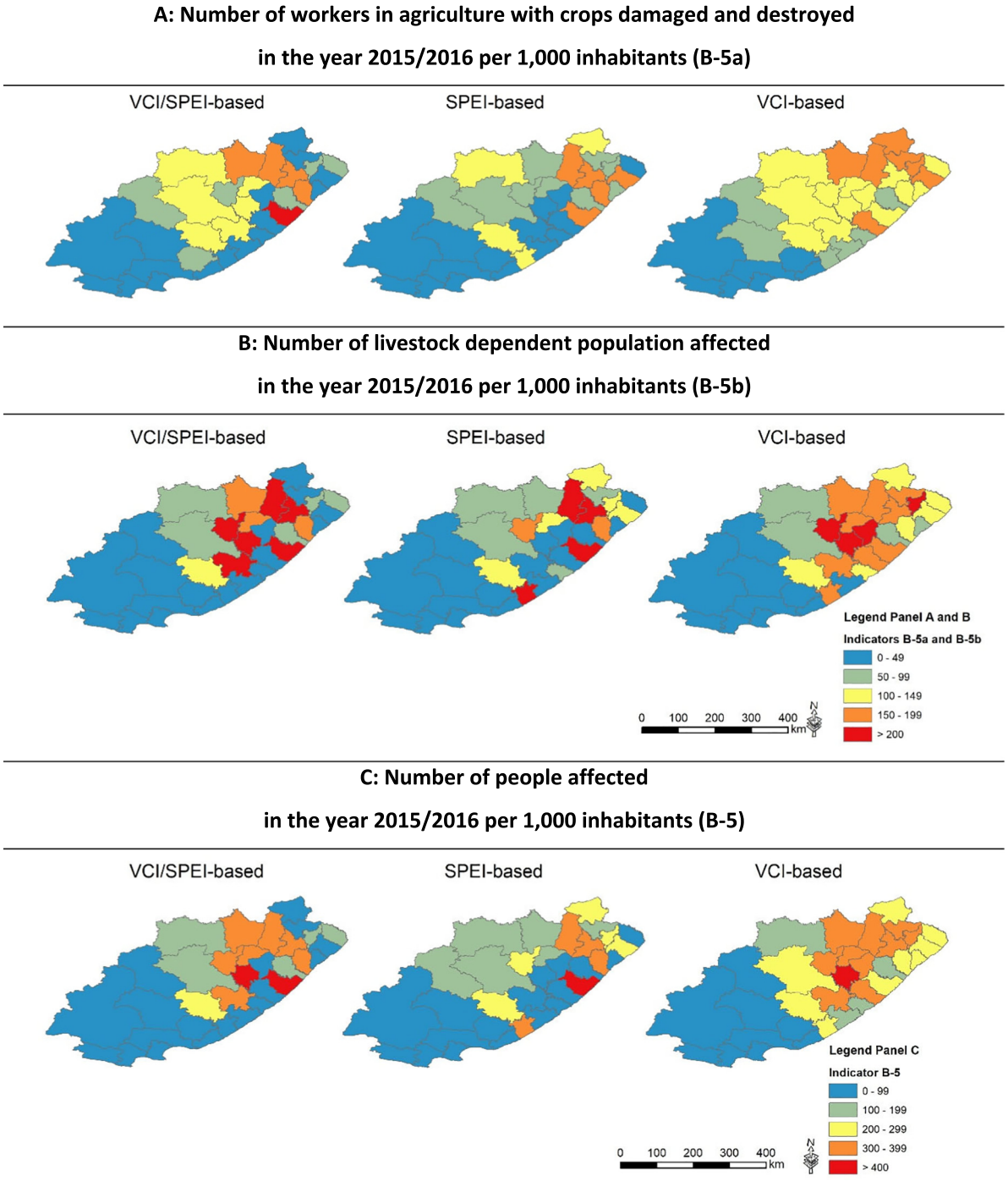

Fig. 4. Results of the measurement of Sendai indicator B5-a (Panel A), B-5b (Panel B) and aggregated indicator B-5 (Panel C) based on the three different drought hazard assessments, namely the combined VCI/SPEI-, SPEI-, and VCI-based assessments.

Table 2
Number of people affected per local municipality due to agricultural drought in 2015/2016 in the Eastern Cape Province, South Africa based on three different hazard assessments (VCI/SPEI, SPEI, VCI) using the geospatial model approach as illustrated in Fig. 3 and the coefficient of variation of the three results at the local municipality level.

District	Local municipality	Population	Number of people affected/1000 inhabitants			Coefficient of Variation
			VCI/SPEI	SPEI	VCI	
Alfred Nzo	Matatiele	203,843	83	245	294	0.53
	Mbizana	281,905	123	0	274	1.04
	Ntabankulu	123,976	122	226	379	0.53
	Umzimvubu	191,620	73	177	319	0.65
Amathole	Amahlathi	122,778	339	0	320	0.87
	Great Kei	38,991	4	99	169	0.91
	Mbhashe	254,909	424	420	294	0.20
	Mnquma	252,390	2	63	327	1.33
	Ngqushwa	72,190	5	352	274	0.86
	Raymond Mhlaba	151,379	255	258	251	0.01
Buffalo City	Buffalo City	755,200	0	44	102	1.05
Cacadu	Blue Crane Route	36,002	91	92	99	0.05
	Dr Beyers Naude	79,291	47	27	69	0.44
	Kouga	98,558	0	10	3	1.22
	Kou-Kamma	40,663	0	20	17	0.87
	Makana	80,390	94	4	54	0.89
	Ndlambe	61,176	0	71	16	1.29
	Sundays River Valley	54,504	77	70	36	0.36
Chris Hani	Emalahleni	119,460	313	229	356	0.22
	Engcobo	155,513	0	0	396	1.73
	Enoch Mgijima	245,975	187	128	209	0.24
	Intsika Yethu	145,372	453	0	432	0.87
	Inxuba Yethemba	65,560	99	102	84	0.10
	Sakhisizwe	63,582	301	169	321	0.31
Joe Gqabi	Elundini	138,141	375	387	346	0.06
	Senqu	134,150	335	148	362	0.41
	Walter Sisulu	77,477	176	156	179	0.07
Nelson Mandela Bay	Nelson Mandela Bay	1,152,115	0	14	4	1.15
O.R.Tambo	King Sabata Dalindyebo	451,710	184	98	195	0.33
	Mhlontlo	188,226	390	390	312	0.12
	Ngquza Hill	278,481	57	285	285	0.63
	Nyandeni	290,390	347	316	251	0.16
	Port St Johns	156,136	0	80	203	1.08

However, the north-eastern part shows a very heterogeneous pattern with overall more affected people in the livestock sector (B-5b) compared to the crop-farming sector (B-5a). Overall, the number of affected people per local municipality ranges between 0 and 453 people per 1000 inhabitants (Table 2).

The resulting maps and detailed results documented in Table 2 show that different hazard products can have a very strong impact on the resulting number of people affected, as some local municipalities range for the same indicator between the minimum and maximum class of affected people. For example, in the Intsika Yethu local municipality, the SPEI-based estimation of B-5 resulted in zero people affected, whereas the VCI-based and combined VCI/SPEI- based assessments yielded 432 and 453 per 1000 people affected, respectively. This variation of results within some local municipalities is further confirmed by the high coefficient of variation, which is documented in Table 2 for the indicator B-5. The highest deviation was detected for Engcobo in the Chris Hani district, while the number of people affected was nearly identically high in Elundini and the Joe Gqabi district based on the three different hazard datasets.

3.2. Evaluation of the calculated Sendai indicator

In the absence of consolidated and structured loss and damage data for the 2015/2016 drought in Eastern Cape province, evaluation of the resulting indicator measures was based on the results of the newspaper content analysis. The resulting evaluation data are (i) number of impacts reported, (ii) severity of impacts reported, and (iii) a composite index derived from the first two measures. The spatial distribution of drought impacts as represented by the evaluation data is illustrated in Fig. 5. Similar to the estimate of the Sendai indicator B-5, the evaluation data show very good agreement on low impacts in the south-western region of Eastern Cape province. In the north-eastern region of the province, the different aspects of evaluation data on number of impacts (Fig. 5 – Panel A) and severity of impacts (Fig. 5 – Panel B) result in different levels of impacts, except for the agreement in the north-eastern corner of the Eastern Cape province. The composite validation index in Fig. 5 – Panel C represents the combined information for evaluating Sendai indicators. The level of detail in the evaluation data did not allow for quantitative information on number of people affected; however, classes of impact severity levels were derived as a basis for statistical evaluation between the estimated Sendai indicators and the evaluation data.

The results of the statistical analysis showed that the agreement between estimated Sendai indicators and the evaluation data from the media content analysis is generally good (Table 3). The Sendai indicators derived from all three different hazard datasets resulted in all cases in a statistically significant (95% to 99% level) positive correlation with impact severity levels derived from evaluation data as indicated by the Spearman rank correlation coefficient and the Cohen Kappa coefficient (Table 3). According to classification by Landis and Koch [37], most resulting Cohen Kappa coefficients correspond to moderate agreement (0.41 to 0.60) with one exception showing a fair agreement (0.39) and two results with substantial agreement (0.63). The interrater agreement is in most cases above 70% (= good agreement), whereas values above 75% are considered to represent excellent agreement [24] (Table 3). The highest and most consistent agreement according to the different statistical measures resulted for the SPEI-based B-5 indicator in relation to the severity of reported impacts (Spearman rank correlation coefficient: 0.61, Interrater Agreement: 81.82% and Cohen Kappa: 0.63). There are a few cases where the results

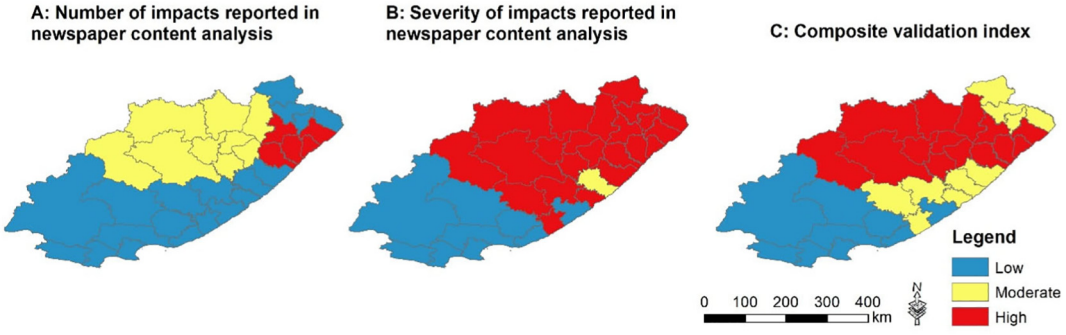

Fig. 5. Results from newspaper content analysis showing in Panel A the number of impacts reported, in Panel B the severity of the reported impacts according to the classification scheme derived by Jordaan [32] and in Panel C the Composite validation index. The classes low, moderate and high indicate whether the respective values of each indicator fall under the first (1–1/3*max), second (>1/3*max - 2/3*max) or third tercile (>2/3*max - max) of the maximum value of each indicator.

Table 3
Results of (a) Spearman rank correlation analysis, (b) the analysis of interrater agreement and the [73] Cohen Kappa coefficient of the B-5 Sendai indicators in reference to the results of the newspaper content analysis. The level of significance of the Spearman rank correlation coefficient and the Cohen Kappa coefficient are indicated with either ** for 99% level of significance or * for 95% level of significance.

	B5 VCI/SPEI	B5 SPEI	B5 VCI
No. of reported impacts	(a) 0.53**	(a) 0.51**	(a) 0.56**
	(b) 75.76%	(b) 75.76%	(b) 69.70%
	(c) 0.51**	(c) 0.51**	(c) 0.39*
Severity of reported impacts	(a) 0.53**	(a) **0.61****	(a) 0.61**
	(b) 75.76%	(b) **81.82%**	(b) 75.76%
	(c) 0.51**	(c) **0.63****	(c) 0.51**
Composite Index	(a) 0.58**	(a) 0.40*	(a) 0.61**
	(b) 75.76%	(b) 81.82%	(b) 75.76%
	(c) 0.51**	(c) 0.63**	(c) 0.51**

of the different statistical measures are not consistent, e.g. due to a comparable low Cohen Kappa coefficient for the relation between VCI-based B-5 indicator and number of reported impacts, or due to the relatively low Spearman rank correlation coefficient for the example of the SPEI-based B-5 indicator. However, in most cases the different statistical measures are in agreement and confirm that the estimated Sendai indicator B-5 shows a good agreement with reference data from the media content analyses regarding loss and damage due to the agricultural drought event.

4. Discussion

This paper presents a geospatial model approach using remote sensing information in combination with spatially explicit statistical data to quantify indicators for monitoring Target B of the SFDRR given the example of agricultural drought in the Eastern Cape province of South Africa. The aim of this methodological innovation is to support countries in monitoring loss and damage due to natural hazards as required for the implementation of the SFDRR. In the following chapter, the geospatial model approach to estimate Sendai indicators, its evaluation, and both opportunities and limitations of the developed model will be discussed in the context of agricultural drought impacts in South Africa.

4.1. Estimating the number of people affected due to agricultural drought

The number of people affected due to a hazardous event is in most cases difficult to define in a precise manner [50], which is already reflected in multiple definitions of the variable “affected people” and therefore has implications for the comparability of loss and damage data. For example, the Emergency Events Database (EM-DAT) defines people affected as “people requiring immediate assistance during a period of emergency” [13], which may include displaced or evacuated people. However, this definition is not applicable to drought as a slow onset hazard, whereby people gradually reach a point at which they require assistance and the predominant focus is on protecting people's livelihoods rather than on morbidity and mortality. In contrast, the definition of DesInventar is documented more broadly as “the number of persons who suffer indirect or secondary effects related to a disaster” [64]. The technical guidance of the *Sendai monitor* discriminates between directly and indirectly affected people, in line with the human loss framework developed by De Groeve et al. [15], whereby directly affected people suffer harm due to the event (e.g. injury, illness, health effects, loss of livelihoods) and indirectly affected people suffer from consequences of the event (e.g. disruption of basic services, changes in the economy) (UNISDR [60]a). The measure of indirectly affected people is of particular relevance for the case of slow onset droughts due to multiple indirect impacts on the economy (e.g. changes of food prices), the environment (e.g. degradation) and the society (e.g. unemployment in agricultural sector). However, the assessment of indirect, cascading effects would require a different approach towards estimating the number of affected people [28], as this can easily extend beyond the regional or country context. Meanwhile, the Sendai Target B considers only the number of directly affected people, which can be assessed by the geospatial model approach presented here.

The model approach presented in this study aimed to “translate” the methods described by the technical guidance [71] into a geospatial procedure which builds on remote sensing data, climate data, land cover and land use data, agricultural statistics and population census data. Given the assumptions made, the indicator B-5a on number of workers in agriculture with crops damaged or destroyed could be directly measured in line with the technical guidance (Eq. (1)) by monitoring vegetation response for cropland using the VCI and/or meteorological conditions using the SPEI and combining this with average workers per hectare derived from agricultural statistics and census data. We argue, however, that due to a different response of individual crop types to water stress [57] this assessment could be improved by disaggregated data on individual crop types in order to apply crop specific loss and damage functions for a more accurate result. Based on the experience of this case study in South Africa, this level of detail is not feasible for the purpose of monitoring loss and damage because crop rotation is a common practice in the region [43] and crop specific maps are not available at the national level with yearly updates. An additional drawback is that our approach was based on census data [54], which does not consider the outmigration from the province between the year 2011 and the time of the assessment in 2015/2016. We therefore expect an overestimation of the number of affected people. Nevertheless, we successfully demonstrated that the Sendai indicator B-5a can be measured by the developed geospatial model approach which directly follows the procedure proposed by the OIEWG-DRR.

However, this direct translation did not hold as true for the measurement of Sendai indicator B-5b, namely the number of workers responsible for and owners of livestock lost, as attributed to agricultural drought. While we could directly determine the average workers per head of livestock at the local municipality level based on agricultural statistics and census data, the measure of livestock lost could only be based on damaged or destroyed grassland as a proxy indicator using VCI and/or SPEI data. The assumption of drought affected grassland being related to affected livestock is considered reasonable for cattle in the context of South Africa; however, there are many more types of livestock that would fall under this indicator but with no documented relation to response of grassland (e.g. chicken). In addition, the households dependent on livestock vary dramatically from communal areas, where farmers are small scale with <15 livestock, to commercial farmers with thousands of livestock per family [30,32]. As the average number of workers per livestock is derived originally from household data (see Fig. 3), we venture that for the case of SA, this diversity could be captured by integrating data on the carrying capacity of grazing into the measure of average workers per livestock.

The remote sensing-based hazard assessment plays a crucial role in this geospatial model approach, as it allows us to assess and monitor the dynamics of drought events. This study used the VCI because this index was found to correspond well with croplands when considered for regional analysis [26]. In addition, a strong correlation between VCI and agricultural production could be found over agricultural areas in Africa and Europe [27,36]. However, in the case of irrigated agriculture, the vegetation condition

does not directly reflect the presence of meteorological drought [22]. VCI provides information on plant health and is thus not directly related to a lack of precipitation. The VCI could therefore overlook farmers who could be economically affected by spending large amounts of their income on irrigation to maintain crop health, without apparent changes in VCI. Furthermore, the VCI only compares a certain day of the year with the exact same day of other years. Thus, shifts in the growing season are not reflected, or even worse, depicted as drought.

With regard to agricultural drought hazard, hydrology also plays an important role, namely when water for irrigated agriculture stems from upstream water catchments which are spatially disjointed from the cropland area [31,33]. The hydrology is not represented by the SPEI and only represented by the VCI in case of green vegetation during a dry period due to irrigation. However, in this research we only explored the meteorological component of droughts by using the SPEI in addition to the vegetation response. The main aim to use different hazard data in this paper was to better understand the sensitivity of the geospatial model approach by investigating the impact of different hazard input data on the resulting number of people affected.

Following the UNDRR technical guidance [71], crops should be assessed whether they are damaged or destroyed. To address this, we followed the classification scheme provided by Jordaan [29] and discriminated between crops damaged and destroyed by setting distinct thresholds (Table 1) in relation to the documented impacts of drought severity classes. As outlined above, we argue that thresholds to assess crops damaged or destroyed might also be different for specific crop types and with regard to their different drought tolerance ability. However, the weighted classification scheme of the VCI applied here aims at integrating a crop-specific sensitivity through time series of phenological metrics. This approach could be improved by integrating crop type specific land cover maps. In addition, we acknowledge that crops damaged as indicated by a VCI between 10 and 40 can result in vast differences of drought impacts, such as changes in production rates and yields. A further confounding factor to the assumed linear relation between the VCI and agricultural drought hazard severity for the assessment of people affected is the phenomenon of land degradation, which appears as green drought due to extensive bush encroachment in South Africa. For the SPEI, crops damaged or destroyed were linked to the thresholds as documented by the SPEI-based drought hazard severity classification [29], which has been tested to result in the respective drought hazard severity classes.

In the absence of a loss and damage database, this geospatial model approach was evaluated for this case study in the EC province based on data from a newspaper content analysis. The methodological approach of this newspaper content analysis ensured that manifested impacts due to the specified drought event were identified and geocoded for a spatially explicit evaluation of the modelled Sendai indicator B-5 in the study area. In addition, the description of impacts could be linked to drought severity classes as described by Jordaan [29]. Thus, quantitative and qualitative information on drought related impacts could be extracted from the media. However, a limitation is that only English newspapers with online access could be analysed in this study and newspapers published in the local languages Xhosa or Afrikaans could not be considered. This means that newspapers are limited mainly to the coastal areas and little coverage of English newspapers is expected in the south western areas of Eastern Cape, where Afrikaans is the main language. In addition, this newspaper content analysis covers only the timeframe from July 2015 until June 2016. However, drought conditions still prevail today, and attribution of impacts to a specific year will become more difficult as time goes on.

4.2. Opportunities and limitations of the geospatial model approach for Sendai monitoring

This geospatial model approach was developed with the overall aim to support countries in the implementation of the SFDRR that have no access to loss and damage databases. In this paper, we demonstrated that the geospatial model approach provides valuable results in reference to data from a newspaper content analysis. Besides the opportunity to enable countries to monitor progress in disaster risk reduction, this geospatial model approach provides the unique opportunity to measure loss and damage in a retrospective manner and with full spatial coverage. Remote sensing data can be used to detect and monitor dynamics of drought hazard severity, also looking back to the beginning of this century and even further, depending on availability of remote sensing data. Thus, the approach presented here is also a unique opportunity for countries to establish the baseline for monitoring progress in disaster risk reduction as required in the SFDRR, in which Target B requires comparison of the measure to a baseline - “aiming to lower the average global figure per 100,000 between 2020–2030 compared to 2005–2015” (UNISDR, 2015).

To the best of our knowledge, this is the first attempt to measure Sendai indicators using a geospatial model approach based on remote sensing data in combination with spatial statistics. Despite an overall good agreement of the results with the impact data from the media, a quantitative validation of number of people affected was not feasible based on the given evaluation data. However, a validation with directly measured loss and damage data is an essential next step in order to understand the level of uncertainties regarding the modelled measure of crops damaged or destroyed, the vulnerability of different livestock and the degree to which grassland can be related to livestock losses. In addition, the coefficient of variation showed that different hazard severity products have a very high impact on the results. This discrepancy could be explained for example by the mismatch regarding the spatial resolution, the different results for irrigated agricultural areas where VCI could still be very high despite a drought, or crop rotation and crop changes that have an impact only on the VCI. The demonstrated high sensitivity of the geospatial model indicates that hazard data need to be selected carefully and used consistently to quantify Sendai indicators on a yearly basis. In contrast, spatial statistical data have very little temporal dynamic information and are generally up to date with the national census. However, as the census usually takes place only every 10 years, this data introduces an additional level of uncertainty given ongoing demographic changes. Against this background, further validation of this approach using loss and damage data is necessary to prove the applicability of the developed model.

The geospatial model approach developed in this study followed the technical guidance developed by the OIEWG-DRR [71]. However, while the conceptualization of the Sendai indicator per its definition by UNISDR [60] only considers elements of hazard and exposure, the framing of disaster risk and impact as provided by the IPCC AR5 more comprehensively includes vulnerability [25], which would be relevant to the number of people affected by agricultural drought. As documented by the equations of the B-5 sub-indicators B-5a and B-5b, the current guidance is to integrate only hazard (e.g. hectares of crops affected) and exposure (e.g. average workers per hectare) (see Fig. 2). Following the definition of the IPCC, however, impact – in this study noted as “number of people affected by agricultural drought in 2015/2016” – is defined as “effects… [that] result from the interaction of … hazardous events occurring within a specific time period and the vulnerability of an exposed society or system” [25]. We argue that the information on vulnerability of the social-ecological system to agricultural drought is essential to complement the impact measure regarding the number of people affected. For instance, if farmers are exposed to a drought hazard yet not vulnerable, they are not affected, whereas high vulnerability could lead to high impacts despite low hazard severity.

5. Conclusion

We present a geospatial model approach which quantifies indicators of the SFDRR for Target B regarding the number of people affected for the example of agricultural drought in the Eastern Cape province of South Africa. The spatial distribution of the modelled number of people affected corresponded very well with reference data from a media content analysis. However, the results of the geospatial model were sensitive to different hazard input data, where the highest and most consistent agreement resulted for the SPEI-based B-5 indicator in relation to the severity of reported

impacts. This geospatial model based on remote sensing and geostatistical data provides a unique opportunity to support countries without information on disaster-related loss and damage in monitoring Target B of the SFDRR. Due to its retrospective nature of assessing loss and damage, even a baseline measure of the indicators can be derived as a reference for monitoring progress. However, the model needs to be further validated where in situ loss and damage data are available. In addition, we argue that characteristics of vulnerability need to be integrated into the UNDRR methodology to better capture the progress made in reducing risk by measuring indicators of Target B. Future research could transfer this model to different hazard contexts for hazard-specific monitoring of loss and damage in order to develop targeted disaster risk reduction measures.

Author contribution

YW, AM and JP designed the geospatial model approach. The quantitative assessment of the model was conducted by AM, KD and YW. The model evaluation was conducted by YW and KD. MD and JCV reviewed the methodological steps of the quantitative assessment. VG and OD developed the remote sensing-based analysis approach and provided VCI data for hazard assessment. YW drafted the manuscript with inputs from all authors. All authors revised and approved the manuscript.

Funding

This work was supported by the German Federal Ministry for Economic Affairs and Energy (BMWi) in the context of the EvIDENz (Earth Observation based information products for drought risk reduction on the national level) project [grant number: 50EE1542].

Declaration of competing interest

The authors declare that they have no known competing financial interests or personal relationships that could have appeared to influence the work reported in this paper.

Acknowledgements

The research is part of the project EvIDENz (grant number: 50EE1542) funded by the German Federal Ministry for Economic Affairs and Energy (BMWi). The authors would like to thank Guido Lüchters for his highly valuable advice on the statistical analyses for the model evaluation and Liliana Marulanda for her support on drafting the Fig. 1.

References

[1] AgriSA, 2016a. A Raindrop in the Drought: Agri SA's Status Report on the Current Drought Crisis 1–27.
[2] Aitsi-Selmi, A., Murray, V., Wannous, C., Dickinson, C., Johnston, D., Kawasaki, A., Stevance, A.S., Yeung, T., 2016. Reflections on a Science and Technology Agenda for 21st Century Disaster Risk Reduction: Based on the Scientific Content of the 2016 UNISDR Science and Technology Conference on the Implementation of the Sendai Framework for Disaster Risk Reduction 2015–20. Int. J. Disaster Risk Sci. 7, 1–29. https://doi.org/10.1007/s13753-016-0081-x.
[3] Anderson K, Ryan B, Sonntag W, Kavvada A, Friedl L. Earth observation in service of the 2030 Agenda for Sustainable Development. Geo-Spatial. Inform Sci 2017;20:77–96. https://doi.org/10.1080/10095020.2017.1333230.
[4] Baudoin MA, Vogel C, Nortje K, Naik M. Living with drought in South Africa: lessons learnt from the recent El Niño drought period. Int J Disaster Risk Reduct 2017;23:128–37. https://doi.org/10.1016/j.ijdrr.2017.05.005.
[5] Begueria S, Vicente-Serrano SM, Reig F, Latorre B. Standardized precipitation evapotranspiration index (SPEI) revisited: parameter fitting, evapotranspiration models, tools, datasets and drought monitoring 3023, 3001–3023; 2014. https://doi.org/10.1002/joc.3887.
[6] Belton S, Stewart TS. Multiple criteria decision analysis. An integrated approach. s. Massachusetts: Kluwer Academic Publishers; 2002.
[7] Bhuiyan C, Saha AK, Bandyopadhyay N, Kogan FN. Analyzing the impact of thermal stress on vegetation health and agricultural drought – a case study from Gujarat. India GIScience Remote Sens 2017;54:678–99. https://doi.org/10.1080/15481603.2017.1309737.
[8] Bhuiyan C, Saha AK, Bandyopadhyay N, Kogan FN. Analyzing the impact of thermal stress on vegetation health and agricultural drought—a case study from Gujarat. India GIScience Remote Sens 2017;54:678–99. https://doi.org/10.1080/15481603.2017.1309737.
[9] Calkins J. Moving forward after Sendai: how countries want to use science, evidence and technology for disaster risk reduction. PLoS Curr 2015;7. https://doi.org/10.1371/currents.dis.22247d6293d4109d09794890bcda1878.
[10] Carrão H, Naumann G, Barbosa P. Mapping global patterns of drought risk: an empirical framework based on sub-national estimates of Hazard. Exposure and Vulnerability Glob Environ Chang 2016;39:108–24. https://doi.org/10.1016/j.gloenvcha.2016.04.012.
[11] Chen S, Zhang L, Liu X, Guo M, She D. The use of SPEI and TVDI to assess temporal-spatial variations in drought conditions in the middle and lower reaches of the Yangtze River basin. China Adv Meteorol 2018;2018. https://doi.org/10.1155/2018/9362041.
[12] Clarke L, Blanchard K, Maini R, Radu A, Eltinay N, Zaidi Z, et al. Knowing what we know – reflections on the development of technical guidance for loss data for the Sendai framework for disaster risk reduction. PLoS Curr 2018:1–13. https://doi.org/10.1371/currents.dis.537bd80d1037a2ffde67d66c604d2a78.
[13] CRED, 2019. The international disaster database - definitions [WWW document]. URL https://www.emdat.be/explanatory-notes (accessed 5.4.19).
[14] DAFF. Abstract of agricultural statistics; 2016.
[15] De Groeve T, Poljansek K, Ehrlich D. Corbane. Current status and best practices for disaster loss data recording in EU Member States: C; 2014. https://doi.org/10.2788/18330.
[16] DEA, 2015. 2013–14 National Land-Cover – 72 classes.
[17] Department of Provincial and Local Government. Disaster Management Act, 2002 (Act No. 57 of 2002). South: Africa; 2005.
[18] Dubovyk O, Landmann T, Erasmus BFN, Tewes A, Schellberg J. Monitoring vegetation dynamics with medium resolution MODIS-EVI time series at sub-regional scale in southern Africa. Int J Appl Earth Obs Geoinf 2015;38:175–83. https://doi.org/10.1016/j.jag.2015.01.002.
[19] FAO. The impact of disasters and crises on agriculture and food security 2018:2018 https://doi.org/978-92-5-130359-7.
[20] GCIS. South Africa Yearbook 2016:2015/16.
[21] GEOTERRAIMAGE. 2013–2014 South African National Land-Cover Dataset; 2014.
[22] Graw V, Ghazaryan G, Dall K, Gómez AD, Abdel-Hamid A, Jordaan A, et al. Drought dynamics and vegetation productivity in different land management systems of Eastern Cape, South Africa-A remote sensing perspective. Sustain 2017;9. https://doi.org/10.3390/su9101728.
[23] Graw V, Ghazaryan G, Schreier J, Gonzalez J, Abdel-Hamid A, Walz Y, et al. Timing is everything - drought classification for risk assessment, in: IEEE Journal of Selected Topics in Applied Earth Observations and Remote Sensing; 2019.
[24] Greve W, Wentura D. Wissenschaftliche Beobachtung - Eine Einführung; 1997.
[25] IPCC. Climate change 2014: Impacts, adaptation, and vulnerability; 2014.
[26] Jeyaseelan AT, Kogan FN. Evaluation of GVI-based indices for drought early warning in India. In: Kogan F, Habib S, Hegde VS, Matsuoka M, editors. International Society for Optics and Photonics; 2006. p. 64120S. https://doi.org/10.1117/12.693929.
[27] Jiao W, Zhang L, Chang Q, Fu D, Cen Y, Tong Q, et al. Evaluating an enhanced vegetation condition index (VCI) based on VIUPD for drought monitoring in the continental United States. Remote Sens (Basel) 2016;8:224. https://doi.org/10.3390/rs8030224.
[28] Johansson M. Experience of data collection in support of the assessment of global progress in the Sendai Framework for Disaster Risk Reduction 2015–2030 – a Swedish pilot study. Int J Disaster Risk Reduct 2017;24:144–50. https://doi.org/10.1016/j.ijdrr.2017.06.008.
[29] Jordaan AJ. Drought indicators and drought classification. Disaster Manag Inst South Africa 2018;2:18–23.
[30] Jordaan AJ. An analysis of the Mngcunube "hands-on" mentorship program for small-scale stock farmers in the eastern cape. South Africa South African J Agric Ext 2012;40:48–57.
[31] Jordaan AJ, Sakulski DM, Muyambu F, Shwababa S, Mdungela N, Phatudi-Mphahlele B, et al. Vulnerability, adaptation to and coping with drought: the case of commercial and subsistence rain fed farming in the eastern cape; 2017.
[32] Jordaan AJ, Sissions D, Blaker J. An Analysis of the Mngcunube "Hands-on" Mentorship Program for Small-scale Stock Farmers in the Eastern Cape. South African Society for Agricultural Extension Officers, in: South African Society for Agricultural Extension Officers - 43rd Annual Congress. Potchefstroom, pp. 178–191; 2009.
[33] Jordaan A, Sakulski D, Muyambo F, Shwababa S, Mdungela N, Phatudi-Mphahlele B, et al. Vulnerability, adaptation to and coping with drought: the case of commercial and subsistence rain fed farming in the Eastern Cape. In: Jordaan A, editor. Vulnerability, adaptation to and coping with drought: The case of commercial and subsistence rain fed farming in eastern cape; 2017 [WRC.].
[34] Kogan F. Application of vegetation index and brightness temperature for drought detection. Adv Sp Res 1995;15:91.
[35] Kogan FN. Remote sensing of weather impacts on vegetation in non-homogeneous areas. Int J Remote Sens 1990;11:1405–19. https://doi.org/10.1080/01431169008955102.
[36] Kogan FN, Kogan FN. Global drought watch from space. Bull Am Meteorol Soc 1997;78:621–36. https://doi.org/10.1175/1520-0477(1997)078<0621:GDWFS>2.0.CO;2.
[37] Landis JR, Koch GG. The measurement of observer agreement for categorical data. Biometric 1977;33:159–74.
[38] Liu Y, Zhou Y, Ju W, Wang S, Wu X, He M, et al. Impacts of droughts on carbon sequestration by China's terrestrial ecosystems from 2000 to 2011. Biogeosciences 2014;11:2583–99. https://doi.org/10.5194/bg-11-2583-2014.
[39] Lorenzo-Alonso A, Utanda Á, Aulló-Maestro M, Palacios M. Earth observation actionable information supporting disaster risk reduction efforts in a sustainable development framework. Remote Sens (Basel) 2019;11:49. https://doi.org/10.3390/rs11010049.

[40] Malherbe J, Dieppois B, Maluleke P, Van Staden M, Pillay DL. South African droughts and decadal variability. Nat Hazards 2016;80:657–81. https://doi.org/10.1007/s11069-015-1989-y.
[41] Manyena B. After Sendai: is Africa bouncing back or bouncing forward from disasters? Int J Disaster Risk Sci 2016;7:41–53. https://doi.org/10.1007/s13753-016-0084-7.
[42] NDMC. Status on Sendai monitoring in South Africa; 2019.
[43] Nel AA. Crop rotation in the summer rainfall area of South Africa. South African J Plant Soil 2005;22:274–8. https://doi.org/10.1080/02571862.2005.10634721.
[44] Ngaka, M.J., 2012. Drought preparedness, impact and response. A case of the Eastern Cape and Free State provinces of South Africa". Jàmbá J. Disaster Risk Stud. 4.
[45] Noort M. Earth observation and sustainable development goals in the Netherlands. Towards More Synergetic Use of Earth Observaation: An Exploratory Study 2017:58.
[46] Pearson L, Pelling M. The UN Sendai framework for disaster risk reduction 2015–2030: negotiation process and prospects for science and practice. J Extrem Events 2015;2:1571001. https://doi.org/10.1142/S2345737615710013.
[47] Schreiner BG, Mungatana ED, Baleta H. Impacts of drought induced water shortages in South Africa: Sector policy briefs; 2018.
[48] Schwalm CR, Anderegg WRL, Michalak AM, Fisher JB, Biondi F, Koch G, et al. Global patterns of drought recovery. Nature 2017;548:202–5. https://doi.org/10.1038/nature23021.
[49] Sehgal VK, Dhakar R. Geospatial approach for assessment of biophysical vulnerability to agricultural drought and its intra-seasonal variations. Environ Monit Assess 2016;188. https://doi.org/10.1007/s10661-016-5187-5.
[50] Serje J. Data sources on hazards. In: Wisner B, Gaillard JC, Kelman I, editors. The Routledge handbook of hazards and disaster risk reduction. New York: Routledge; 2012. p. 179–90.
[51] StataCorp. Stata: Release 14. Statistical software; 2015.
[52] StatSA, 2016b. Provinces at a glance [WWW document]. URL http://cs2016.statssa.gov.za/wp-content/uploads/2016/06/CS-2016-Provinces-at-a-glance.pdf (accessed 4.29.19).
[53] StatSA, 2013. Census 2011: agricultural households - key highlights. Pretoria.
[54] StatSA. Agricultural households municipal data per province; 2011 [Eastern Cape].
[55] StatSA. Census of commercial agriculture. Eastern Cape: Provincial statistics for selected products; 2007; 2007.
[56] StatsSA, 2019. Mid-year population estimates.
[57] Steduto, P., Hsiao, T.C., Fereres, E., Raes, D., 2012. Crop yield response to water (No. 66), FAO Irrigation and Drainage Paper. Rome.
[58] Svoboda M, LeComte D, Hayes M, Heim R, Gleason K, Angel J, et al. The drought monitor. Bull Am Meteorol Soc 2002;83:1181–90. https://doi.org/10.1175/1520-0477-83.8.1181.
[59] Tang LL, Cai X Bin, Gong WS, Lu JZ, Chen XL, Lei Q, et al. Increased vegetation greenness aggravates water conflicts during lasting and intensifying drought in the Poyang Lake watershed, China. Forests 2018:9. https://doi.org/10.3390/f9010024.
[60] UN, 2017. New urban agenda.
[61] UN. Report of the open-ended intergovernmental expert working group on indicators and terminology relating to disaster risk reduction; 2016 [United Nations General Assembly].
[62] UN, 2015a. Resolution adopted by the General Assembly on 3 June 2015 - 69/283. Sendai Framework for Disaster Risk Reduction 2015b–2030.
[63] UN. Transforming our world: The 2030 agenda for sustainable development, seventieth United Nations general assembly. New York: New York; 2015.
[64] UNDRR, 2019. DesInventar Sendai - definition of basic effects [WWW document]. URL https://www.desinventar.net/effects.html (accessed 5.5.19).
[65] UNFCCC, 2015. Paris Agreement, 21st Conference of the Parties. https://doi.org/FCCC/CP/2015/L.9.
[66] UNISDR, 2019a. Integrated monitoring of the global targets of the Sendai Framework and the Sustainable Development Goals [WWW document]. Prev. Web. URL https://www.preventionweb.net/sendai-framework/sendai-framework-monitor/common-indicators (accessed 1.9.19).
[67] UNISDR, 2019b. We monitor [WWW document]. URL https://www.unisdr.org/we/monitor (accessed 4.7.19).
[68] UNISDR, 2019c. Measuring implementation of the Sendai framework - global targets reporting years 2015–2018 [WWW document]. URL https://sendaimonitor.unisdr.org/ (accessed 1.15.19).
[69] UNISDR, 2019d. South Africa disaster & risk profile [WWW document]. URL https://www.preventionweb.net/countries/zaf/data/ (accessed 2.21.19).
[70] UNISDR, 2018. DesInventar statistics. Bonn.
[71] UNISDR. Technical guidance for monitoring and reporting on Progress in achieving the global targets of the Sendai framework for disaster risk reduction; 2017.
[72] UNISDR. Disaster-Related Data for Sustainable Development - Sendai Framework Data Readiness Review 2017:1–77.
[73] UNISDR, 2015. Sendai Framework for Disaster Risk Reduction 2015–2030. Third World Conf. Disaster Risk Reduction, Sendai, Japan, 14–18 March 2015c. https://doi.org/A/CONF.224/CRP.1.
[74] Vicente-Serrano SM, Beguería S, López-Moreno JI. A multiscalar drought index sensitive to global warming: the standardized precipitation evapotranspiration index. J Climate 2010;23:1696–718. https://doi.org/10.1175/2009JCLI2909.1.
[75] Vogt, J., Barbosa, P., de Jager, A., Naumann, G., Cammalleri, C., Spinoni, J., Magni, D., Mazzeschi, M., Arias Muñoz, C., Lavaysse, C., McCormick, N., 2018. The Global Drought Observatory (GDO): Integrating Hazard, Exposure and Vulnerability for Risk Analysis and Emergency Response, in: AGU Fall Meeting Abstracts. pp. H42C-01.
[76] Wahlström M. New Sendai framework strengthens focus on reducing disaster risk. Int J Disaster Risk Sci 2015;6:200–1. https://doi.org/10.1007/s13753-015-0057-2.
[77] Wang R, Cherkauer K, Bowling L. Corn response to climate stress detected with satellite-based NDVI time series. Remote Sens (Basel) 2016;8. https://doi.org/10.3390/rs8040269.
[78] Wilhite DA. Drought as a natural hazard: conceptions and definitions. Drought A Glob Assess 2000:111–20.
[79] World Bank, 2019. DataBank - world development indicators [WWW document]. URL https://databank.worldbank.org/data/reports.aspx?source=2&type=metadata&series=SP.POP.TOTL (accessed 5.4.19).